Available online at www.sciencedirect.com
SCIENCE DIRECT®
International Journal of Thermal Sciences 44 (2005) 491–498
International Journal of Thermal Sciences
www.elsevier.com/locate/ijts

Absorption of water vapour in the falling film of water–(LiBr + LiI + $LiNO_3$ + LiCl) in a vertical tube at air-cooling thermal conditions

Mahmoud Bourouis *, Manel Vallès, Marc Medrano, Alberto Coronas

Centro de Innovación Tecnológica en Revalorización Energética y Refrigeración, CREVER, Universitat Rovira i Virgili, Autovía de Salou, s/n, 43006, Tarragona, Spain

Received 7 January 2004; received in revised form 30 August 2004; accepted 10 November 2004

Abstract

In air-cooled water–LiBr absorption chillers the working conditions in the absorber and condenser are shifted to higher temperatures and concentrations, thereby increasing the risk of crystallisation. To develop this technology, two main problems are to be addressed: the availability of new salt mixtures with wider range of solubility than water–LiBr, and advanced absorber configurations that enable to carry out simultaneously an appropriate absorption process and an effective air-cooling. One way of improving the solubility of LiBr aqueous solutions is to add other salts to create multicomponent salt solutions. The aqueous solution of the quaternary salt system (LiBr + LiI + $LiNO_3$ + LiCl) presents favourable properties required for air-cooled absorption systems: less corrosive and crystallisation temperature about 35 K lower than that of water–LiBr.

This paper presents an experimental study on the absorption of water vapour over a wavy laminar falling film of an aqueous solution of (LiBr + LiI + $LiNO_3$ + LiCl) on the inner wall of a water-cooled smooth vertical tube. Cooling water temperatures in the range 30–45 °C were selected to simulate air-cooling thermal conditions. The results are compared with those obtained in the same experimental set-up with water–LiBr solutions.

The control variables for the experimental study were: absorber pressure, solution Reynolds number, solution concentration and cooling water temperature. The parameters considered to assess the absorber performance were: absorber thermal load, mass absorption flux, degree of subcooling of the solution leaving the absorber, and the falling film heat transfer coefficient.

The higher solubility of the multicomponent salt solution makes possible the operation of the absorber at higher salt concentration than with the conventional working fluid water–LiBr. The absorption fluxes achieved with water–(LiBr + LiI + $LiNO_3$ + LiCl) at a concentration of 64.2 wt% are around 60 % higher than those of water–LiBr at a concentration of 57.9 wt%.

Keywords: Absorption; Falling film absorber; Air-cooled absorber; water–LiBr; water–(LiBr + LiI + $LiNO_3$ + LiCl)

1. Introduction

The water–lithium bromide (LiBr) absorption systems which are mainly used in large cooling capacity applications (industry, large buildings, etc.) require water from cooling towers to reject heat. The middle and low capacity residential and commercial systems are dominated by the more compact air-cooled compression systems. Absorption machines should be air-cooled in order to become competitive at lower capacities.

In the last decade, many Japanese and Korean firms that manufacture absorption machines jointly with the gas utilities have initiated projects to develop air-cooled absorption technology with water–lithium bromide [1–3]. The main problem in the development of these air-cooled machines is the large heat exchange surface required, which involves more expensive and larger equipment. Moreover, for heat to

* Corresponding author. Phone: +34977540205, fax: +34977542272.
E-mail address: mahmoud.bourouis@urv.net (M. Bourouis).

1290-0729/$ – see front matter
doi:10.1016/j.ijthermalsci.2004.11.009

Nomenclature

A	heat transfer area	m^2
c_p	specific heat	$kJ{\cdot}kg^{-1}{\cdot}K^{-1}$
D	diameter	m
g	gravitational acceleration	$m{\cdot}s^{-2}$
h	convective heat transfer coefficient	$W{\cdot}m^{-2}{\cdot}K^{-1}$
j	mass absorption flux	$kg{\cdot}m^{-2}{\cdot}s^{-1}$
H	specific enthalpy	$kJ{\cdot}kg^{-1}$
m	mass flow rate	$kg{\cdot}s^{-1}$
Nu	Nusselt number, $= \frac{h_s\delta}{\lambda}$	
P	pressure	kPa
Q	heat rate	W
Re	Reynolds number; $= \frac{4\Gamma}{\mu} = \frac{4\delta\cdot v\rho}{\mu}$	
T	temperature	°C
U	overall heat transfer coefficient	$W{\cdot}m^{-2}{\cdot}K^{-1}$
X	concentration (weight % LiBr)	

Greek symbols

δ	film thickness, $= (\frac{3\mu\Gamma}{\rho^2 g})^{1/3}$	
Γ	$m/\pi D_i$ mass flow rate per unit of wetted perimeter	$kg{\cdot}m^{-1}{\cdot}s^{-1}$
λ	thermal conductivity	$W{\cdot}m^{-1}{\cdot}K^{-1}$
μ	dynamic viscosity	$N{\cdot}s{\cdot}m^{-2}$
ν	kinematic viscosity	$m^2{\cdot}s^{-1}$
ρ	density	$kg{\cdot}m^{-3}$

Subscripts

Abs	absorber
ae	cooling water
e	external
eq	equilibrium
HE	heat exchanger
i	internal
in	inlet
M	mass
out	outlet
p	wall
Rot	flowmeter
s	solution
SUB	subcooling
v	vapour phase

be dissipated to ambient air, the working conditions in the absorber and condenser are shifted to higher temperatures and concentrations, thereby increasing the risk of crystallisation.

If this new equipment is to be technologically developed, various well-defined problems need to be addressed. The first problem is that of the availability of new salt mixtures with a wider range of solubility. The second is that the absorber must permit new configurations that enable an appropriate absorption process and an effective air-cooling to be carried out simultaneously. Lastly, we have to bear in mind the distribution of the solution in the absorber and the other components of air-cooled absorption equipment, so that a more effective and compact final product can be designed.

One way of improving the solubility of the LiBr aqueous solution is to add other salts to create multicomponent salt solutions. The criteria for selecting one of these new salt mixtures for air-cooled absorption chillers should not only include the increase in the solubility range but also other aspects of machine operation such as: vapour pressure, viscosity, corrosivity, thermal and chemical stability, etc. Among the mixtures proposed in recent years, water–(LiBr + LiI + $LiNO_3$ + LiCl) stands out because of their excellent thermophysical properties. For the sake of illustration, at a typical salt concentration of 62.0 wt% the crystallisation temperature is around 30 °C lower than that of a LiBr solution [4]. The presence of lithium chloride decreases the vapour pressure, lithium iodide and lithium nitrate improve the solubility and lithium nitrate reduces corrosion in the system. In fact, this multicomponent solution has been used to develop several air-cooled prototypes for absorption air conditioning [1,2].

Most of the experimental studies about falling film absorption process in vertical tubes with a water–LiBr solutions [5–12] have been carried out with the falling film on the outer surface of smooth tubes, and also with absorption heat dissipation by means of cooling water at relatively low temperatures (20–35 °C). Only Kurosawa et al. [13] have experimentally studied the falling film absorption process inside smooth and rough vertical tubes. They performed the experiments with a water–LiBr solution at a concentration of 55.0 wt% and a cooling water temperature in the range 19–32 °C. The falling film heat transfer coefficients were in the range 0.4–2.0 $kW{\cdot}m^{-2}{\cdot}K^{-1}$.

Yoon et al. [14] published experimental data of heat and mass transfer in a helical absorber using the new working fluid, and concluded that the heat and mass flux performances of the solution were around 2 and 5% higher than those of the water–LiBr solution.

In a previous work, an air-cooled absorber was designed to be incorporated in a water chiller prototype. The absorber consisted of vertical finned tubes with the falling film and the water vapour flowing concurrently inside the tubes. Then, the absorption process was studied inside a single water-cooled vertical tube absorber at air-cooling thermal conditions using the conventional working fluid water–LiBr. In this paper, the results achieved with the multicomponent salt solution in the same experimental set-up are presented and compared with those of water–LiBr [15].

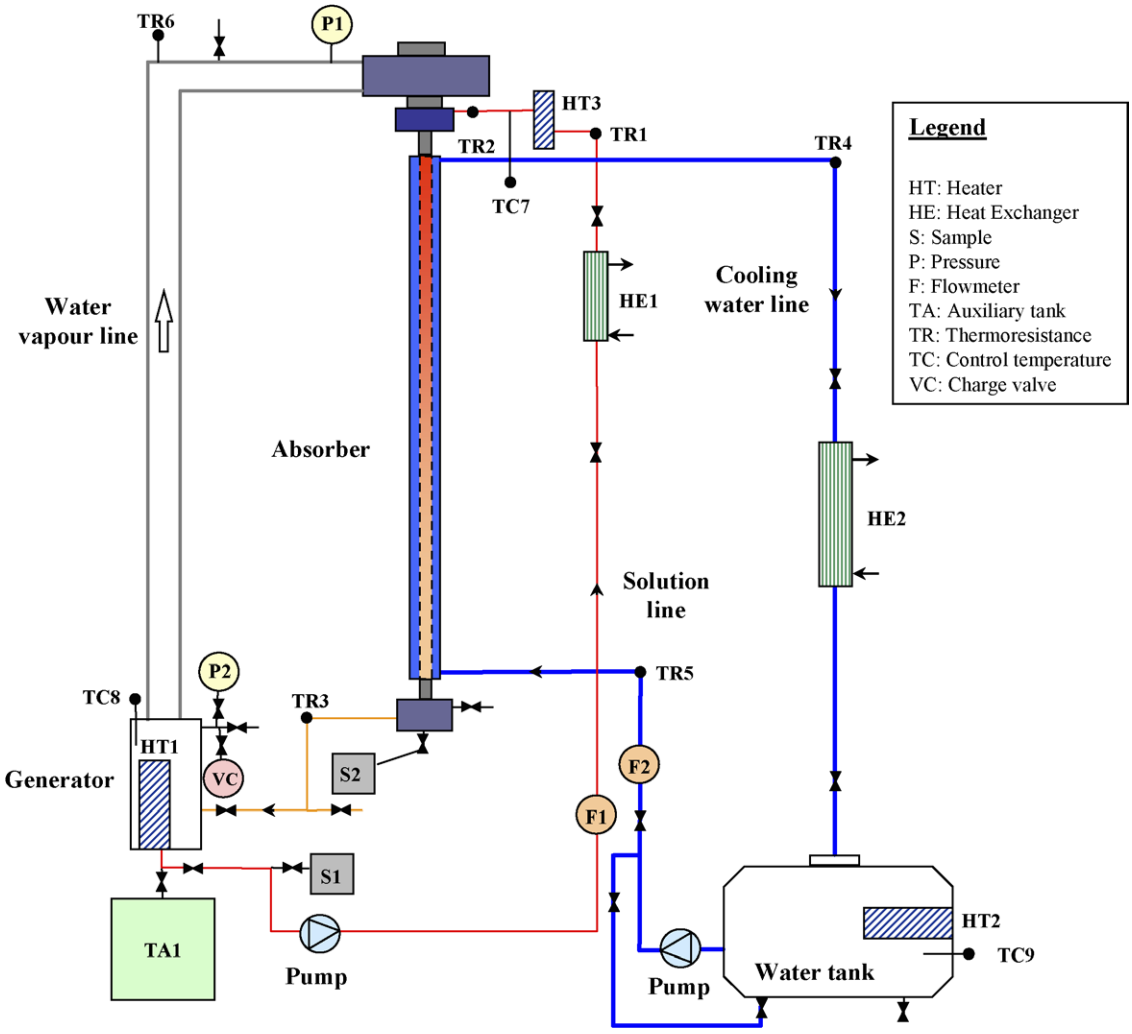

Fig. 1. Schematic diagram of the experimental set-up.

2. Description of experimental set-up

The main components of the experimental set-up shown in Fig. 1 were the absorber, the generator, the solution loop, the cooling water loop, and the control and measurement devices. The system was designed to operate in a continuous mode.

The absorber consisted of two stainless steel concentric tubes of 1.5 m length, the liquid and vapour distributors at the top, and a weak solution collector at the bottom. The inner absorber tube had an inside diameter of 22.1 mm and a polished inner wall surface. The falling film solution and the water vapour from the generator flowed down this surface concurrently. Cooling water flowed countercurrently in the annular space. The weak solution leaving the absorber was collected in a small receiver at the bottom before returning to the generator.

To distribute the solution flow entering the absorber, there was a plastic cylindrical filter located concentrically to the absorber tube. The water vapour from the generator enters the absorber through a ring distributor. At the top and the bottom of the absorber, two concentric peepholes were mounted to check the proper wetting of the falling film.

The generator consisted of a stainless steel cylinder and three electrical heaters on the bottom with an overall power of 4 kW. The working pressure of the system was controlled indirectly by means of the temperature control of the solution in the generator.

The salt solution loop was formed by a magnetic coupling gear pump with a variable speed controller, a precision flowmeter (F1), a water cooled heat exchanger cooler (HE1) and a heater tank (HT3). The pump moved the solution from the bottom to the top of the absorber at a height of about 3 meters. The strong solution leaving the pump was cooled down with tap water in the heat exchanger (HE1) and was heated up in the electric heater (HT3) to the set inlet temperature before entering the absorber.

The cooling water loop was formed by a water tank, a centrifugal pump, a flowmeter (F2), the absorber jacket, and a heat exchanger (HE2). This heat exchanger cooled the hot water leaving the absorber below the absorber inlet tempera-

ture so that it could be controlled by a 4 kW heater provided in the water tank.

The experimental set-up had two auxiliary tanks. The auxiliary tank (TA1) was used to drain the generator in case of operation problems. The other auxiliary tank (TA2) was used to collect and weigh the condensed water that was separated when the working concentration of the strong solution was increased.

The purge system for removing non-absorbable gases consisted of a liquid ring vacuum pump and a liquid nitrogen cold trap. The system was operated at an acceptable leak rate below 2×10^{-8} kPa·m^3·s^{-1}.

The inlet and outlet solutions could be sampled in two pre-evacuated flasks (S1 and S2) and their concentrations determined using a precision Anton Paar densimeter.

3. Experimental measurements

Table 1 shows the measured experimental variables and the accuracy of the corresponding measurement instruments.

3.1. Test conditions

The variables considered for the parametric study of the absorber performance were the cooling water temperature, the absorber pressure, the solution flow rate and the inlet solution concentration. The temperature of the strong solution entering the absorber was kept between 5 and 10 °C above the inlet cooling water temperature.

3.2. Performance parameters

The parameters selected to assess the absorber performance were: the absorber thermal load, the mass absorption flux, the outlet degree of subcooling and the falling film heat transfer coefficient. The thermophysical properties were taken from a property database, which contains the most updated literature correlations [4].

The *absorber thermal load* is defined as the heat released in the absorber which is removed by the cooling water and was calculated as:

$$Q_{\text{Abs}} = m_{\text{ae}} C p_{\text{ae}} (T_{\text{ae,out}} - T_{\text{ae,in}}) \tag{1}$$

The *mass absorption flux* j is the absorbed mass flow rate per unit mass transfer surface A_M. It was calculated by matching the heat fluxes in solution and water sides. The solution side absorber load was expressed by:

$$Q_{\text{Abs}} = m_{s,\text{in}} H_{s,\text{in}}(T_{s,\text{in}}, X_{s,\text{in}}) - m_{s,\text{out}} H_{s,\text{out}}(T_{s,\text{out}}, X_{s,\text{out}}) + j A_M H_v(T_v, P_{\text{Abs}}) \tag{2}$$

The above equation was solved numerically, taking into account the overall and partial mass balances of the solution in the absorber.

The *degree of subcooling* of the solution leaving the absorber is the deviation of the actual outlet solution temperature from the equilibrium solution temperature at the absorber pressure and the outlet solution concentration. High subcooling values indicate that the solution could have absorbed more refrigerant and is an indication of the ineffectiveness of the absorber.

$$\Delta T_{\text{SUB}} = T_{\text{eq,out}} - T_{s,\text{out}} \tag{3}$$

The *falling film heat transfer coefficient* is given by:

$$h_s = \left[\left(\frac{1}{U} - \frac{D_e}{2\lambda_p} \ln \frac{D_e}{D_i} - \frac{1}{h_{\text{ae}}} \right) \frac{D_i}{D_e} \right]^{-1} \tag{4}$$

A relatively high heat transfer coefficient (~8.5 kW·m^{-2}·K^{-1}) on the cooling water side was maintained by working at a Reynolds number of 6000. As the heat transfer resistance on water side was rather low (2–10% of total resistance), the uncertainty in the evaluation of the falling film coefficient was reduced.

The overall heat transfer coefficient was given by:

$$U = \frac{Q_{\text{Abs}}}{A \Delta T} \tag{5}$$

The driving potential for heat transfer independent of the outlet conditions was chosen:

$$\Delta T = T_{\text{eq,in}} - T_{\text{ae,in}} \tag{6}$$

Table 1
Measured variables and accuracy of the corresponding instruments

Measured variable	Instrument	Accuracy
Volumetric flow rate of strong solution before entering the absorber, $m_{s,\text{in}}$	Flowmeter	$\pm 1.0 \times 10^{-6}$ m^3·s^{-1}
Volumetric flow rate of cooling water, m_{ae}	Flowmeter	$\pm 1.4 \times 10^{-5}$ m^3·s^{-1}
Temperature of weak solution leaving the absorber, $T_{s,\text{out}}$	Pt100 probe	±0.025 °C
Temperature of strong solution entering the absorber, $T_{s,\text{in}}$	Pt100 probe	±0.025 °C
Absorber pressure, P_{Abs}	Piozoresistive pressure transducer	±0.035 kPa
Temperature of inlet cooling water, $T_{\text{ae,in}}$	Pt100 probe	±0.025 °C
Temperature of outlet cooling water, $T_{\text{ae,out}}$	Pt100 probe	±0.025 °C
Temperature of solution leaving the cooler HE1, T_{HE1}	Pt100 probe	±0.025 °C
Temperature of water vapour, T_v	Pt100 probe	±0.5 °C
Concentration of strong solution entering the absorber, $X_{s,\text{in}}$	Anton Paar densimeter	±0.1% weight
Concentration of weak solution leaving the absorber, $X_{s,\text{out}}$	Anton Paar densimeter	±0.1% weight

For the calculation of the mass transfer coefficient the mean logarithmic concentration difference was used.

An uncertainty analysis of the obtained experimental absorber parameters was carried out. The average relative error of the thermal absorber load, mass absorption flux, falling film heat transfer coefficient, degree of subcooling was around 7, 15, 9 and 3%, respectively.

4. Comparison of the absorption process with the multicomponent salt and lithium bromide solution in a vertical falling film absorber

To characterise the absorption process of water vapour in the aqueous solution of $LiBr + LiI + LiNO_3 + LiCl$, a sensitive study of the operation of a falling film vertical absorber with both multicomponent and LiBr solutions was carried out.

In the following sub-sections, the effect of the absorber pressure, solution flow rate, and cooling water temperature on the absorber behaviour are discussed for both water–LiBr and water-multicomponent salt solutions. The solution inlet concentration to the absorber was 57.9% by weight for the former, and 61.0 and 64.2 wt% for the later as its solubility is higher.

4.1. Effect of the absorber pressure

The driving force for mass transfer through the vapour–liquid interface can be expressed as the difference between the partial pressure of water vapour in the vapour phase (which is equal to total pressure if non-absorbable gases are negligible) and the vapour pressure of water–salt solution at a given temperature and concentration. Thus, the higher the absorber pressure, the greater is the potential for vapour transfer to the falling film.

Fig. 2 shows how the thermal load increases with the absorber pressure. At a relatively low solution flow rate (Reynolds number of 90) the absorber load is in the range 0.4–1.0 kW for water–LiBr at 57.9 wt% when the absorber pressure is increased from 1.0 to 2.1 kPa. The same trend is observed with the multicomponent salt solution at a concentration of 61.0 wt%, but it is more pronounced at 64.2 wt% for which the absorber load is in the range 0.65–1.20 kW.

For the results presented in the next sections, the absorber pressure was set to 1.3 kPa, which corresponds to an evaporator temperature of around 11 °C. These operating conditions are typical for a direct expansion evaporator and an air-cooled absorber.

4.2. Effect of the solution flow rate

Although the experiments were carried out with similar volumetric flows for the two working fluids, the higher viscosity of the multicomponent salt solution reduces significantly the corresponding Reynolds number. Thus, the

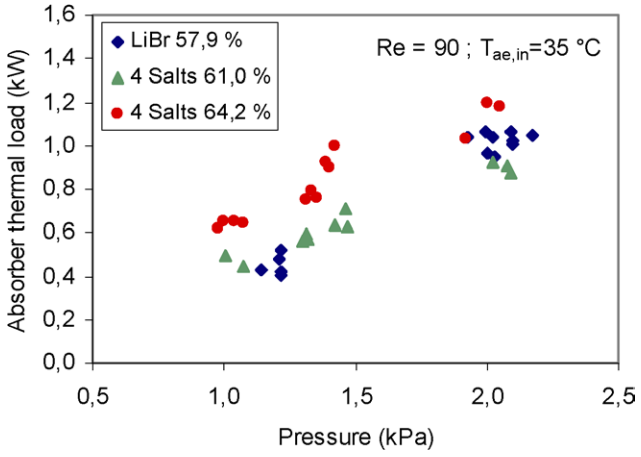

Fig. 2. Effect of absorber pressure on absorber thermal load.

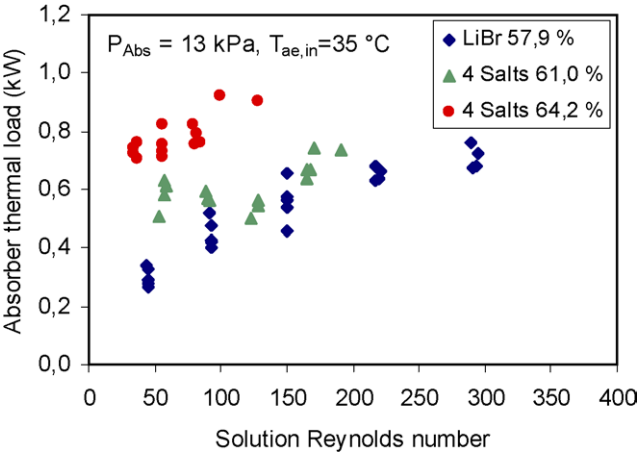

Fig. 3. Effect of solution Reynolds number on absorber thermal load.

maximum Reynolds numbers achieved with this multicomponent salt solution were only around 130 at a concentration of 64.2 wt% and about 170 at 61.0 wt%. However, with the conventional working fluid water–LiBr the maximum Reynolds number was about 330. Thus, the comparison of the results achieved with both solutions is possible in the common Reynolds number range, that is, 75–175. All these Reynolds numbers fall within the wavy-laminar falling film regime ($25 < Re < 1000$), which mostly prevails in commercial absorption chillers.

Fig. 3 shows how the solution Reynolds number affects the absorber thermal load for both solutions. The thermal load with the multicomponent salt solution at a concentration of 61.0 wt% was similar to that of water–LiBr solution at 57.9 wt%. When concentrating the multicomponent solution to 64.2 wt% the thermal load increases considerably compared with that of water–LiBr solution. For example, at a Reynolds number of 105 the increase is around 60%. The absorption mass flux of the two diluted solutions are similar, while that of the concentrated multicomponent solution is always higher as shown in Fig. 4.

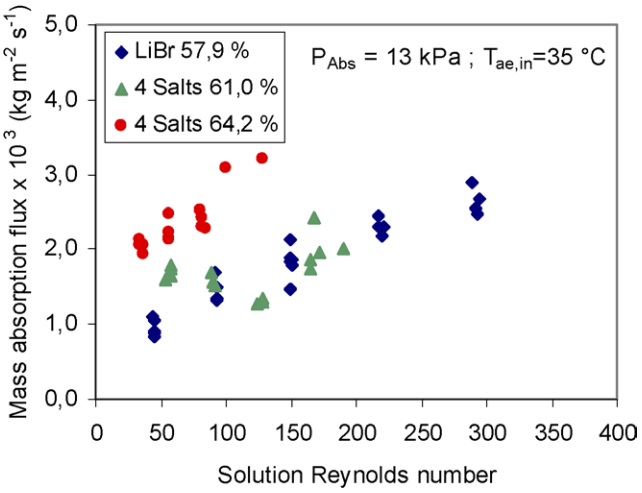

Fig. 4. Effect of solution Reynolds number on mass absorption flux.

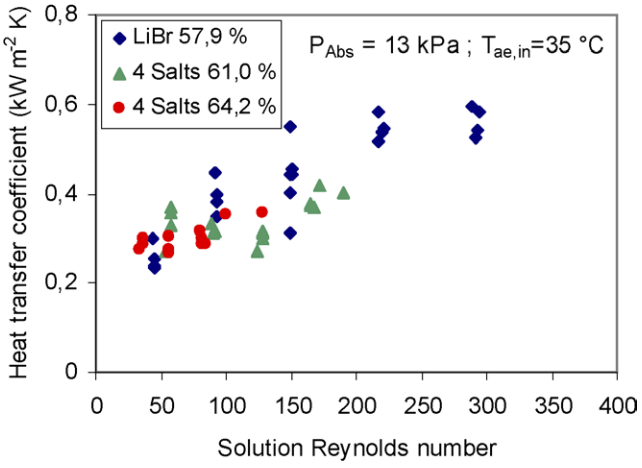

Fig. 5. Effect of solution Reynolds number on falling film heat transfer coefficient.

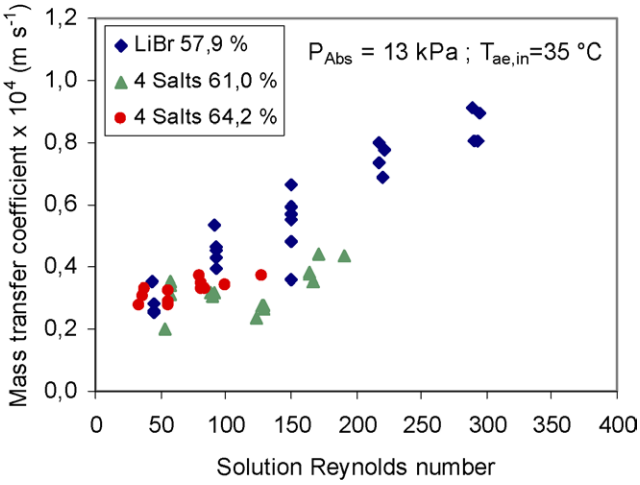

Fig. 6. Effect of solution Reynolds number on mass transfer coefficient.

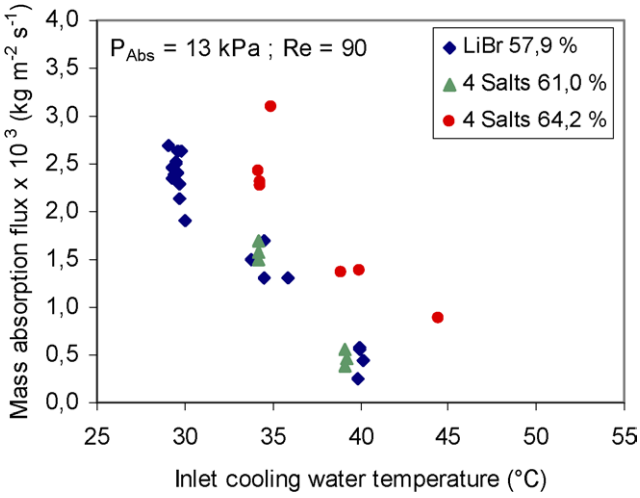

Fig. 7. Effect of cooling water temperature on mass absorption flux.

Figs. 5 and 6 show the film-side heat transfer coefficient and the mass transfer coefficient respectively as a function of the solution Reynolds number, at an absorber pressure of 1.3 kPa and a cooling water temperature of 35 °C. The heat and mass transfer coefficients increase almost linearly for both solutions, and have slightly lower values for the multicomponent salt solution.

In the common range of Reynolds numbers, the film heat transfer coefficient shows similar results for both solutions and increases with Reynolds number from 0.2 to 0.6 $kW \cdot m^{-2} \cdot K^{-1}$. The numerical values of the mass transfer coefficient for water–LiBr solution range between 2.6–9.0 $\times 10^{-5}$ $m \cdot s^{-1}$ while those of the multicomponent salt solution range between 2.7–3.7 $\times 10^{-5}$ $m \cdot s^{-1}$ at a concentration of 64.2 wt%, and between 2.0–4.4 $\times 10^{-5}$ $m \cdot s^{-1}$ at 61.0 wt%.

4.3. *Effect of the cooling water temperature*

The cooling water mass flow rate was set to a constant value corresponding to a Reynolds number around 6000. This resulted in that the resistance to heat transfer on the water-side was low and that the temperature difference between the entrance and the exit to the absorber was large enough for the absorber thermal load to be calculated with acceptable accuracy.

The inlet concentration of the solution directly affects the driving mass transfer potential. The higher the concentration, the lower the solution vapour pressure, and therefore the higher the mass transfer driving potential. However, in practice, the restricted solubility of the water–LiBr solution does not allow operation at concentrations over 62.0% by weight. The new multicomponent salt solution makes it possible to shift this limit to around 68.0 wt%, which establishes a much higher mass transfer driving potential.

As shown in Fig. 7, the absorption mass flux achieved with the multicomponent salt solution at a concentration of 61.0 wt% is similar to that of water–LiBr solution. When concentrating the multicomponent solution to 64.2 wt% the mass flux increases considerably compared with that of water–LiBr solution. For example, at a cooling water tem-

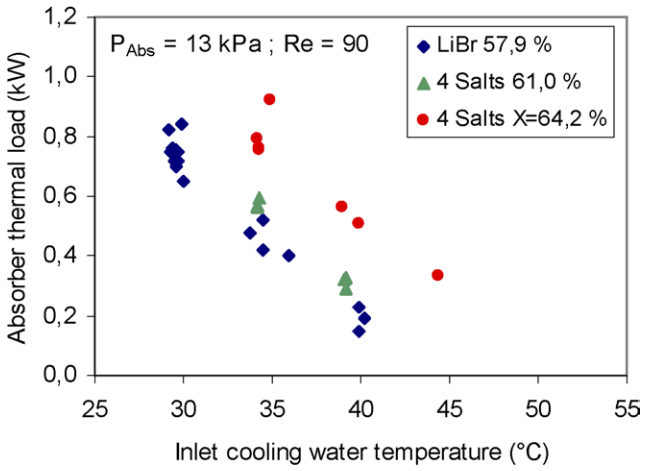

Fig. 8. Effect of cooling water temperature on absorber thermal load.

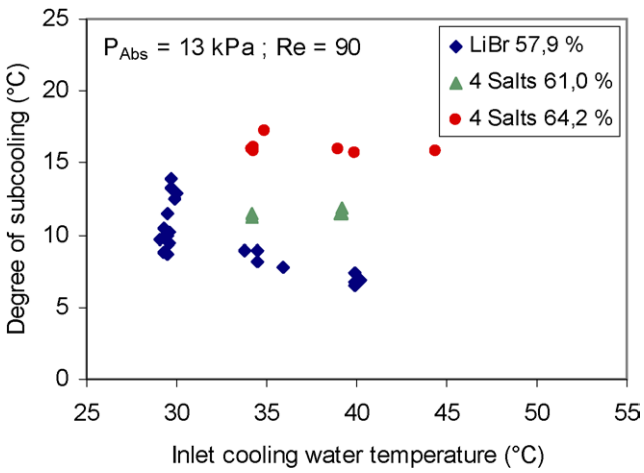

Fig. 9. Effect of cooling water temperature on subcooling of outlet solution.

perature of 35 °C and a solution Reynolds number of 90, the mass absorption flux is around 1.5×10^{-3} kg·m^{-2}·s^{-1} for water–LiBr solution and the multicomponent salt solution at 61.0 wt%, whereas it is about 2.5×10^{-3} kg·m^{-2}·s^{-1} for the later at 64.2 wt%. At a cooling water temperature of 40 °C the absorption mass flux is reduced to 0.5×10^{-3} and 1.5×10^{-3} kg·m^{-2}·s^{-1}, respectively. The absorber thermal load shows a similar trend as it can be observed in Fig. 8.

Fig. 9 shows the influence of cooling water temperature on the degree of subcooling of the solution leaving the absorber. At the same absorber pressure and cooling water temperature the degree of subcooling of the multicomponent salt solution increases with the concentration and is always higher than that of water–LiBr. The trend observed for the degree of subcooling shows that when the driving potential for mass transfers increases more water vapour is absorbed but the absorber efficiency is lower.

5. Conclusions

Experiments on the absorption of water vapour over a wavy laminar falling film of the multicomponent salt solution water–(LiBr + LiI + $LiNO_3$ + LiCl) (5 : 1 : 1 : 2 by mole) on the inner wall of a smooth tube have been carried out at two salt concentrations: 61.0 and 64.2 wt%. The results are compared with those achieved in the same experimental set up with the conventional working fluid water–LiBr at a concentration of 57.9 wt%. The main conclusions of this study are:

- The higher solubility of the multicomponent salt solution makes possible the operation of the absorber at higher salt concentration than with the conventional working fluid water–LiBr. At a typical salt concentration of 62 wt% the temperature of crystallisation of the multicomponent salt solution is about 30 °C lower.
- The mass absorption flux and thermal load have similar numerical values for the multicomponent salt solution at 61.0 wt% and water–LiBr solution at 57.9 wt%, while the film side heat and mass transfer coefficients are slightly lower and the subcooling of the solution leaving the absorber is higher for the former.
- At an absorber pressure of 1.3 kPa, a cooling water temperature of 35 °C, and a solution Reynolds number in the range 75–175 (wavy laminar regime of falling film), the observed ranges of mass absorption flux, thermal load, heat and mass transfer coefficients, and degree of subcooling are 0.001–0.002 kg·m^{-2}·s^{-1}, 0.3–0.7 kW, 0.2–0.5 kW·m^{-2}·K^{-1}, 2.0–6.5 $\times 10^{-5}$ m·s^{-1}, and 7–12 °C, respectively, for water–LiBr at 57.9 wt% and water–(LiBr + LiI + $LiNO_3$ + LiCl) at 61.0 wt%.
- When concentrating the multicomponent salt solution to 64.2 wt%, the absorber thermal load and mass absorption flux (at a solution Reynolds number of 125) increase by 28 and 50%, respectively, and the degree of subcooling increases till 15–17 °C in comparison with the corresponding values achieved with water–LiBr at 57.9 wt%. However, heat and mass transfer coefficients hardly change.

Acknowledgements

The authors would like to thank the Spanish Programme for Technical Research (PROFIT-2000, number 314) for subsidising this work.

References

[1] Y. Yoshida, R. Kawakami, H. Kawaguchi, K. Ooka, O. Ooishi, Development of an air-cooled absorption packaged air conditioning unit, in: Proc. Gas Research Conference, Cannes, France, vol. IV, 1995, pp. 106–115.
[2] S. Tongu, Y. Makino, Practical operating of small-sized air-cooled double-effect absorption chiller-heater by using lithium bromide and

aqueous, in: Proc. Absorption Heat Pump Conference, New Orleans, Louisiana, vol. 31, ASME, 1993, pp. 125–132.

[3] T. Okano, Y. Asawa, M. Fujimoto, N. Nishiyama, Y. Sanai, Development of an air-cooled absorption refrigerating machine using a new working fluid, in: Proc. Absorption Heat Pump Conference, New Orleans, Louisiana, vol. 31, ASME, 1993, pp. 311–314.

[4] M. Medrano, Desarrollo de un absorbedor tubular vertical enfriado por aire para un climatizador de absorción de agua–bromuro de litio (Development of an air-cooled vertical tube absorber for an absorption air conditioner using water–lithium bromide), Ph.D. Thesis, Universitat Rovira i Virgili, Tarragona, Spain, 2001.

[5] K.J. Kim, Performance evaluations of LiCl and LiBr for absorber design applications in the open cycle absorption refrigeration system, in: Proc. Absorption Heat Pump Conference, Montreal, Canada, vol. II, 1996, pp. 769–778.

[6] K.J. Kim, N.S. Berman, S.C. Chaud, B.D. Wood, Absorption of water vapour into falling films of aqueous lithium bromide, Internat. J. Refrig. 18 (1995) 486–494.

[7] K.J. Kim, S. Kulankara, K.E. Herold, C. Miller, Heat transfer additives for use in high temperature applications, in: Proc. Absorption Heat Pump Conference, Montreal, Canada, vol. I, 1996, pp. 89–97.

[8] I. Morioka, M. Kiyota, R. Nakao, Absorption of water vapor into a film of aqueous solution of LiBr falling along a vertical pipe, JSME Internat. J. B 36 (2) (1993) 351–356.

[9] A. Beutler, L. Hoffmann, G. Alefeld, K. Gommed, K. Grossmann, A. Shavit, Experimental investigations of heat and mass transfer in film absorption on horizontal and vertical tubes, in: Proc. Absorption Heat Pump Conference, Montreal, Canada, vol. I, 1996, pp. 409–419.

[10] D.S. Sheehan, P. Prescott, H. Perez-Blanco, Investigation of additive effectiveness with infrared sensor dynamic surface tension measurements, in: Proc. Absorption Heat Pump Conference, Montreal, Canada, vol. I, 1996, pp. 75–82.

[11] WA. Miller, M. Keyhani, The correlation of simultaneous heat and mass transfer experimental data for aqueous lithium bromide vertical falling film absorption, J. Solar Energy Engrg. Trans. ASME 123 (1) (2001) 30–42.

[12] S. Kulankara, Effect of enhancement additives on the absorption of water vapor by aqueous lithium bromide, Ph.D. Thesis, University of Maryland, College Park, 1999.

[13] S. Kurosawa, Y. Nagaoka, A. Yoshida, O. Masato, Y. Kunugi, Development of air-cooled gas-fired absorption water chiller-heater, in: Working Fluids and Transport Phenomena in Advanced Absorption Heat Pumps (Annex 14), vol. 2, The IEA Heat Pump Center, 1990, pp. 9-41–42.

[14] J.I. Yoon, H.S. Lee, C.G. Moon, E. Kim, J.D. Kim, B.B. Saha, Heat and mass transfer characteristics of a helical absorber using LiBr and $LiBr + LiI + LiNO_3 + LiCL$ solutions, in: Proc. Experimental Heat Transfer, Fluid Mechanics, and Thermodynamics Conference, Thessaloniki, Greece, vol. 3, 2001, pp. 2303–2308.

[15] M. Medrano, M. Bourouis, A. Coronas, Absorption of water vapour in the falling film of water–lithium bromide inside a vertical tube at air-cooling thermal conditions, Internat. J. Thermal Sci. 41 (2002) 891–898.